Journal of Applied Polymer Science

Effects of Epoxidized Natural Rubber (ENR-50) and Processing Parameters on the Properties of NR/EPDM Blends Using Response Surface Methodology

Noraiham Mohamad,[1] Juliana Yaakub,[1] Jeefferie Abd Razak,[1] Mohd Yuhazri Yaakob,[1] Mohammed Iqbal Shueb,[2] Andanastuti Muchtar[3]

[1]Faculty of Manufacturing Engineering, Universiti Teknikal Malaysia Melaka, Hang Tuah Jaya, 76100, Durian Tunggal, Melaka, Malaysia

[2]Composites and Polymer Blends Group, Radiation Processing Technology Division, Malaysian Nuclear Agency, Bangi, 43000 Kajang, Malaysia

[3]Faculty of Engineering, Universiti Kebangsaan Malaysia, 43600, UKM Bangi, Selangor, Malaysia

Correspondence to: N. Mohamad (noraiham@utem.edu.my)

ABSTRACT: The effects of epoxidized natural rubber (ENR-50) and processing parameters on the properties of natural rubber/ethylene–propylene–diene rubber (NR/EPDM; 70 : 30 phr) blends were studied. The compounds were prepared by melt compounding method. Using response surface methodology of two-level full factorial, the effects of ENR-50 contents (−1 : 5 phr; +1 : 10 phr), mixing temperature (−1 : 50°C; +1 : 110°C), rotor speed (−1 : 40 rpm; +1 : 80 rpm), and mixing time (−1 : 5 min; +1 : 9 min) in NR/EPDM blends were evaluated. Cure characteristics and tensile properties were selected as the responses. The significance of factors and its interaction was analyzed using ANOVA and the model's ability to represent the system was confirmed using the constant of determination, R^2 with values above 0.90. It was found that the presence of ENR-50 has the predominant role on the properties of NR/EPDM blends. The addition of ENR-50 significantly improved cure characteristics and tensile strength up to 5.12% and 6.48% compared to neat NR/EPDM blends, respectively. These findings were further supported by swell measurement, differential scanning calorimetry, and scanning electron microscopy. © 2014 Wiley Periodicals, Inc. J. Appl. Polym. Sci. **2014**, *131*, 40713.

KEYWORDS: compatibilization; crosslinking; differential scanning calorimetry; elastomers; morphology

Received 14 November 2013; accepted 11 March 2014
DOI: 10.1002/app.40713

INTRODUCTION

Blending two or more types of elastomers is a useful method to attain materials with additional properties together with minimum loss of their original properties.[1,2] In fact, the blends can be easily modified to meet performance and cost objectives required by the present markets. In recent years, natural rubber (NR) has been exploited in a wide range of applications such as in tires, engine mounts, seals, and gaskets,[3–5] due to its superior strength, fatigue resistance, high resilience, and low level of strain sensitivity. Hence, it is popular for many applications involving high stress and cyclic flexing. However, the poor resistance of NR to oxygen, ozone, and heat makes it unsuitable for many high-performance applications.[6]

In contrast, ethylene–propylene–diene rubber (EPDM) has saturated hydrocarbon backbones which imparts good weathering oxidation and chemical resistance.[7] The incorporation of a suitable amount of EPDM into NR can become technologically important as the excellent outdoor properties of EPDM, and the good elastic properties of NR are combined.[8,9] However, the difference in olefin concentration of EPDM and NR results in a cure rate incompatible blends which usually exhibit phase separated morphology and poor interfacial adhesion between the phases, thus resulting in poor mechanical properties.[10]

Consequently, many attempts have been done to promote cure compatibility of rubber blends, such as halogenation of EPDM in solution, modification of EPDM with reactive chemicals, for example, maleic anhydride,[11] functionalization of EPDM with mercapto groups as a compatibilizing agent in NBR/EPDM blends,[12] NR/EPDM blends,[12] and brominated EPDM blends with NR.[13] Another method is by adding the third polymeric component into immiscible phases that could interact either chemically or physically with the host materials.[14] For example, the homogeneity of highly incompatible acrylonitrile–butadiene rubber (NBR)/EPDM blends has been greatly improved by the

Table I. Typical Formulation

Ingredient	Loading (phr)[a]
NR (SMR 20)	70
EPDM	30
ENR-50	5-10
Zinc oxide	5.0
Stearic acid	2.0
Sulfur	1.5
MBTS[b]	1.0
TMTD[c]	0.3
6PPD[d]	2.0

[a] Parts per hundred rubber
[b] 2,20-dithiobis (benzothiazole).
[c] Tetramethylthiuram disulfide.
[d] *N*-(1,3-Dimethylbutyl)-*N*′-phenyl-*p* phenylenediamine.

addition of chlorinated polyethylene and transpolyoctenylene rubber,[15] and this might be attributed to the polar group effect by the third component which increases the interaction between immiscible phases.

There is a considerable number of articles investigating epoxidized natural rubber (ENR) as compatibilizer in various polymer blends.[16–18] Margaritis and Kalfoglou[19] and Noriman et al.[20] have reported that the incorporation of ENR into rubber blends can develop finer dispersed phase in the matrix and show improvement in processability, stiffness, resilience, good damping, and wet grip performance because of the presence of polar groups in ENR. Based on this observation, ENR was chosen as a third component compatibilizer to improve the interaction between NR and EPDM in this study.

Conversely, processing the parameters are also important factors to be optimized, since they may affect overall properties and reliability of the end products.[21] To prepare NR/EPDM blends using an internal mixer, processing parameters such as mixing temperature, mixing time, and rotor speed need to be optimized. Optimization through statistical and mathematical approach is a useful technique for it is less time consuming and able to detect true optimum of the factor.[22] Response surface methodology (RSM) is a commonly used technique due to its reliability.[23–25] It allows simultaneous evaluation for a number of factors and eliminates the need for a large number of independent experiments which are otherwise required in a conventional one-factor-at-a-time or trial-and-error approach.[26]

Although numerous efforts were adopted to overcome the incompatibility in NR/EPDM blends, literature which investigates the combination effects of ENR-50 as a third component compatibilizer and processing parameters on the properties of NR/EPDM blends is scarce. Thus, this study reports the findings in term of polynomial mathematical model to represent relationships between compatibilizer and processing parameters (temperature, rotor speed, and time) with respect to the resultant cure characteristics and tensile properties. The findings were further supported by swelling behavior, thermal and morphological characteristics of the blend. This observation later contributed to the improvement in compatibility of NR/EPDM blends.

EXPERIMENTAL

The compound formulation used in the present study is shown in Table I. NR, SMR 20 grade was supplied by Rubber Research Institute of Malaysia. Ethylene propylene diene monomer used was EPDM Buna®EPT 9650, procured from Lanxess Corp. with ENB content of 6.5 ± 1.1 wt %; ethylene content $= 53 \pm 4$ wt %; and Mooney viscosity UML $(1 + 8)$ at $150°C = 60 \pm 6$. ENRs under the trade name ENR-50 with 53% epoxidization was supplied by Malaysian Rubber Board. The average Mooney viscosity measured at ML (1 ± 4) 100°C was 67, and the average specific gravity at approximately 25°C was 0.9366. Other compounding ingredients such as sulfur, zinc oxide, and stearic acid were purchased from System/Classic Chemical Sdn Bhd.; tetramethyl thiuram disulfide (Perkacit-TMTD) and 2,20-dithiobis (benzothiazole; Perkacit-MBTS) was acquired from Perkacit; *n*-(1,3-dimethylbutyl)- *n*′-phenyl-*p*-phenylenediamine (6PPD) were supplied by Flexsys America.

Experimental Design

Design experiments were performed using Design Expert software (Statistics Made Easy, version 6.0.10, Stat-Ease, Minneapolis, MN). Two-level factorial design experiment was utilized in this study. Independent variables in this study were ENR-50 (X_1), temperature (X_2), rotor speed (X_3), and time (X_4) with levels of variables as shown in Table II. The dependent variables consist of the value of scorch time, t_{s2} (Y_1); cure time, t_{90} (Y_2); maximum torque, M_H (Y_3); torque difference, $M_H - M_L$ (Y_4); tensile strength, T_S (Y_5); modulus at 100% elongation, M_{100} (Y_6); modulus at 300% elongation, M_{300} (Y_7), and elongation at break, E_B (Y_8) According to this method, there were 19 experiments with three replications at center point. Factorial design matrix used for this study is listed in Table III. Using RSM with minimum number of experiments, it is possible to obtain quantitative equations for the effects of compatibilizer and processing parameters on the properties of the blends. An application of this method in rubber field has also been reported by Mohamad et al.[22] and Kukreja et al.[27]

Samples Preparation and Cure Characteristic Assessment

The compounding process was performed according to ASTM D 3192[27] using a Haake internal mixer working with a combination of parameters determined by the Design Expert software 6.0.10 based on two level factorial designs. First, NR, EPDM, and ENR-50 were masticated for 1 min before all ingredients except sulfur and accelerators were added. Finally, sulfur and accelerators were added and mixed for 1 min before the mixture

Table II. Levels of Variables

ENR-50 (X_1; Phr)	Temperature (X_2; °C)	Rotor speed (X_3; rpm)	Time (X_4; min)
5 (−1)	50 (−1)	40 (−1)	5 (−1)
7.5 (0)	80 (0)	60 (0)	7 (0)
10 (+1)	110 (+1)	80 (+1)	9 (+1)

Table III. 2^4 Factorial Design Matrix

Experiments	Coded variable			
	ENR (X_1)	Temperature (X_2)	Rotor speed (X_3)	Time (X_4)
1	−1	−1	−1	−1
2	+1	−1	−1	−1
3	−1	+1	−1	−1
4	+1	+1	−1	−1
5	−1	−1	+1	−1
6	+1	−1	+1	−1
7	−1	+1	+1	−1
8	+1	+1	+1	−1
9	−1	−1	−1	+1
10	+1	−1	−1	+1
11	−1	+1	−1	+1
12	+1	+1	−1	+1
13	−1	−1	+1	+1
14	+1	−1	+1	+1
15	−1	+1	+1	+1
16	+1	+1	+1	+1
17	0	0	0	0
18	0	0	0	0
19	0	0	0	0

was dumped and left to cool at room temperature. The cure characteristics of the compounds were obtained using a Monsanto moving die rheometer (MDR 2000). Samples of the respective compounds were tested at 140°C. The rubber compounds were subsequently compression molded at 140°C using a hot press based on the respective cure time, t_{90} which is in accordance with ASTM D 2084.

Tensile Testing

Dumbbell-shaped samples were cut from the molded sheets using a die cutter. Then, tensile testing of the vulcanized samples was performed according to BS 6746 using Universal Testing Machine (Toyoseiki Strograph) at room temperature and at a cross-head speed of 500 mm/min. At least seven samples were tested for every set of experiments to ensure a high confidence level.

Analysis Techniques

Swell Measurement. The swell measurement was performed according to ISO 1817. The cured specimens with dimensions of 30 × 5 × 2 mm^3 were weighed using an electric balance, followed by immersion in a toluene for 72 h at room temperature (25°C) in a dark environment. After the conditioning period, the swollen specimens were taken out and weighed again. The specimens were then dried in an oven at 60°C until constant weight was obtained.

$$\text{Swelling percentage } (\%) = \frac{W_1 - W_2}{W_2} \times 100 \quad (1)$$

Where W_1 is the mass of samples after the swelling while W_0 is the initial mass of samples before the immersion in toluene. The crosslink density was measured by applying Flory–Rehner equation, whereby the molecular weight between crosslink (M_c) and the crosslink density (V_c) or the concentration of elasticity effective chains can be calculated based on the swelling test results. This parameter includes the true chemical crosslinks and physical crosslinks such as chain entanglements and loops. The Flory–Rehner equations are illustrated in eqs. (2–4) below

$$M_c = \frac{-\rho_P V_S V_r^{1/3}}{\ln(1-V_r) + V_r + \chi V_r^2} \quad (2)$$

$$V_R = \frac{1}{1+Q_m} \quad (3)$$

$$V_c = \frac{1}{2M_c} \quad (4)$$

where ρ is the density of the rubber, V_s is the molar volume of the solvent (toluene), V_r is the volume fraction of the swollen rubber, χ is the interaction parameter of the rubber, and Q_m is the weight increase of the NR/EPDM blends in toluene. The following constant values were used to determine the degree of crosslinking density of NR/EPDM blends.

V_s (toluene) 106.35 cm^3/mol; χ of NR = 0.393; χ of EPDM = 0.49

Differential Scanning Calorimetry. Differential scanning calorimetry (DSC) measurement was performed using Perkin–Elmer DSC-7 analyzer. The 5–10 mg sample was scanned from −65 to 100°C at a scan rate of 10°C/min under nitrogen atmosphere.

Scanning Electron Microscopy. Scanning electron microscopy (SEM), model EVO-50 from Zeiss, was used to analyze the fracture surfaces concerning morphological properties of the blends. Samples were placed onto aluminum stubs and sputter coated with thin layer of gold, about 20-mm thickness; prior to scanning to avoid electrostatic charging and poor resolution during examination.

RESULTS AND DISCUSSION

From the experimental findings, an approximate polynomial relationship for dependent variables (response) was obtained. The result of this design was used to fit a first-order polynomial eq. (5), which included all interaction terms

$$Y = \beta_o + \beta_1 x_1 + \beta_2 x_2 + \beta_3 x_3 + \ldots + \beta_k x_k + \varepsilon \quad (5)$$

where Y is the predicted response; β is the coefficient values; x is the independent variables, and ε is a random error. In this study, $k = 4$ was used because there were four independent variables involved. The mathematical relationship connecting the two variables and the response from eq. (5) becomes

$$Y = B_o + B_1 X_1 + B_2 X_2 + B_3 X_3 + B_4 X_4 + B_{12} X_1 X_2 + B_{13} X_1 X_3 + B_{14} X_1 X_4 + B_{23} X_2 X_3 + B_{24} X_2 X_4 + B_{34} X_3 X_4 \quad (6)$$

where Y is the predicted response; B_o is the offset term; B_1, B_2, B_3, and B_4 are the linear coefficients; B_{12}, B_{13}, B_{14}, B_{23}, B_{24}, and B_{34} are the cross-product coefficient; and X_1, X_2, X_3, and X_4 are the independent variables. The model selected for each response was based on the highest priority in accordance with the polynomial level and the lowest P-value. From the RSM, a regression equation for the selected model for the response, Y was derived.

Table IV. Regression Equations for Different Responses

Responses	R^2	Adjusted R^2	Equation of the models
Scorch time (t_{s2})	0.9848	0.9741	$Y_1 = 2.77 + 0.014\ X_1 - 0.72\ X_2 - 0.072\ X_4 + 0.065\ X_1X_2 + 0.061\ X_1X_4 - 0.04\ X_2X_4 + 0.07\ X_1X_2X_4$
Cure time (t_{90})	1.0000	0.9997	$Y_2 = 4.01 - 0.19\ X_1 - 0.88\ X_2 - 0.012\ X_3 - 0.049\ X_4 + 0.12\ X_1X_2 - 1.25 \times 10^{-3}\ X_1X_3 + 0.072\ X_1X_4 - 0.013\ X_2X_3 - 0.016\ X_2X_4 - 1.0 \times 10^{-2}\ X_3X_4 - 0.02\ X_1X_2X_3 + 0.069\ X_1X_2X_4 - 0.027\ X_1X_3X_4 - 0.011\ X^2X^3X^4 + 0.046\ X_1X_2X_3X_4$
M_H	0.9738	0.9363	$Y_3 = 18.83 + 0.82\ X_1 + 0.31\ X_2 - 0.051\ X_3 + 0.36\ X_4 + 0.37\ X_1X_2 - 0.17\ X_1X_3 - 0.027\ X_2X_3 + 0.14\ X_2X_4 - 0.11\ X_3X_4 + 0.17\ X_2X_3X_4$
$M_H - M_L$	0.9775	0.9618	$Y_4 = 12.94 + 1.23\ X_1 - 0.61\ X_2 + 0.18\ X_4 + 0.72\ X_1X_2 + 0.41\ X_1X_4 - 0.22\ X_2X_4 + 0.17\ X_1X_2X_4$
T_S	0.9551	0.9045	$Y_5 = 23.91 + 2.03\ X_1 - 2.69\ X_2 - 0.67\ X_3 + 0.59\ X_4 + 0.57\ X_1X_2 - 0.72\ X_1X_3 - 0.97\ X_2X_3 - 1.14\ X_2X_4 - 0.95\ X_3X_4$
M_{100}	0.9992	0.9931	$Y_6 = 2.56 + 0.057\ X_1 - 0.093\ X_2 - 0.071\ X_3 - 0.026\ X_4 + 0.071\ X_1X_2 + 0.033\ X_1X_3 + 0.082\ X_1X_4 - 0.065\ X_2X_3 - 0.048\ X_2X_4 - 0.027\ X_3X_4 + 0.059\ X_1X_2X_3 + 0.061\ X_1X_2X_4 + 0.077\ X_1X_3X_4 - 0.046\ X_2X_3X_4 + 0.047 \times 10^{-5}\ X_1X_2X_3X_4$
M_{300}	0.9987	0.9889	$Y_7 = 3.94 + 0.0.025\ X_1 - 0.07\ X_2 - 0.012\ X_3 - 0.021\ X_4 + 0.04\ X_1X_2 - 6.25 \times 10^{-4}\ X_1X_3 + 0.065\ X_1X_4 - 0.043\ X_2X_3 - 0.02\ X_2X_4 - 0.025\ X_3X_4 + 0.025\ X_1X_2X_3 + 0.04\ X_1X_2X_4 - 0.062\ X_1X_3X_4 - 0.025\ X_2X_3X_4 + 0.023\ X_1X_2X_3X_4$
E_B	0.9923	0.9738	$Y_7 = 3.94 + 0.0.025\ X_1 - 0.07\ X_2 - 0.012\ X_3 - 0.021\ X_4 + 0.04\ X_1X_2 - 6.25 \times 10^{-4}\ X_1X_3 + 0.065\ X_1X_4 - 0.043\ X_2X_3 - 0.02\ X_2X_4 - 0.025\ X_3X_4 + 0.025\ X_1X_2X_3 + 0.04\ X_1X_2X_4 - 0.062\ X_1X_3X_4 - 0.025\ X_2X_3X_4 + 0.023\ X_1X_2X_3X_4$

In Table IV, regression model for each response are presented. All terms are included in each equation.

This mathematical relationship represents the quantitative effects of the independent variables and their interaction effects to the response. Positive values reflect effects that lead to optimization whereas negative values are factors which provide opposite effect on the response. The R^2 values indicate the degree of agreement between the experimental results with those predicted by model. The R^2 values for all responses are obtained in the range of 0.90–0.99 which are very close to union ($R^2 = 1$); almost 100% of the variation in the overall system was presented by the model. This indicates that the regression model is accurate in describing and predicting the pattern of significance for each factor studied.[28]

Interaction Between Variables for Cure Characteristics and Tensile Properties of the Blends

Scorch time (t_{s2}) is the time offset during which a rubber compound can be workable at given temperature before curing begins.[29] In this study, an optimal value of t_{s2} is needed because when t_{s2} is too low, the rubber compound has inadequate time to fill up the mold, thereby producing products that do not meet specifications. Figure 1(a) depicts the response surface for the variation on scorching time as a function of ENR-50 and temperature. According to the response surface plot, the t_{s2} increased as ENR-50 content increased from 5 to 10 phr. This might be attributed to the combination of primary and secondary accelerators which considerably delayed the scorch time, which improved the processing safety toward efficient vulcanization system. Conversely, t_{s2} value decreased as mixing temperature increased. At high temperature, more thermal energy was supplied to overcome the activation energy of the vulcanization. According to Sadequl et al.,[30] the shorter scorch time is observed as the temperature increases. This is due to sufficient thermal energy to cause faster curing at higher temperature. Moreover, the mobility of rubber chain increases which increases the probability for crosslinking to occur.

Figure 1(b) demonstrates the cure time (t_{90}) versus ENR-50 and mixing temperature in 3D surface plot. The t_{90} value decreased with the increase of ENR-50 contents together with temperature factors in the blends. This result might be related to the presence of epoxide groups which induced the *in situ* formation of compatibilizing interchain copolymer of EPDM and NR. Hence, there were strong interactions at the interface between the rubber phases. Similar condition occurred for t_{90} when temperature was increased from 50 to 110°C. This observation could be due to the higher glass transition temperature for ENR-50 compared to NR. This is evident from DSC observation in Figure 4.

Mittal et al.[31] stated that maximum torque (M_H) is commonly considered as a representative of the compound modulus. As shown in Figure 1(c), the M_H value of NR/EPDM blends increased as ENR-50 content increased. Hence, good interaction in the blends was attributed to reactive compatibilization between polar groups of ENR-50 with carbon–carbon double bond of the unsaturated rubber. Meanwhile, torque difference ($M_H - M_L$) is a measure of dynamic shear modulus which indirectly relates to the crosslink density of the blends[32] which

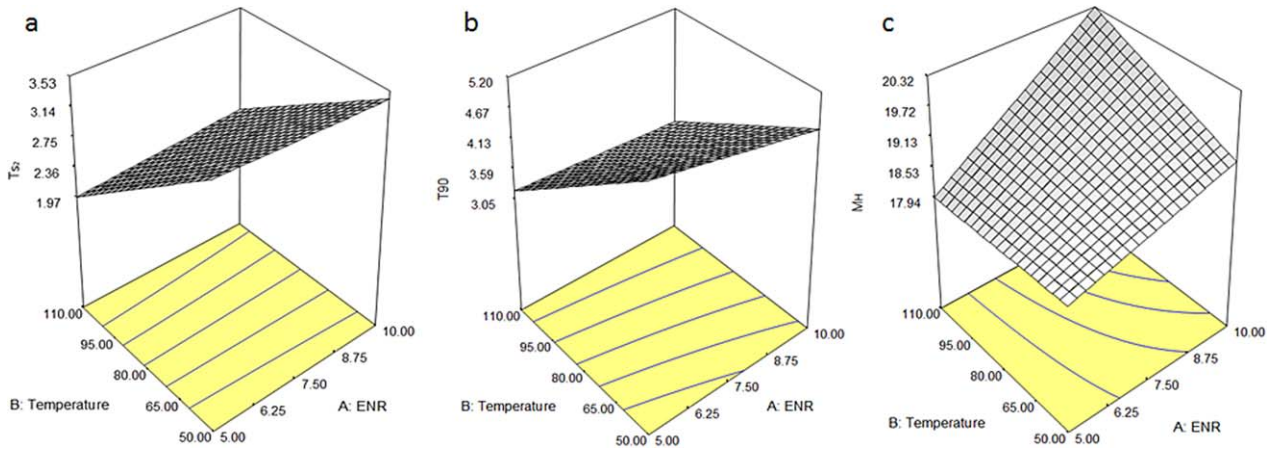

Figure 1. Response surface plot showing variation in (a) scorch time (ts_2); (b) cure time (t_{90}); and (c) maximum torque (M_H). [Color figure can be viewed in the online issue, which is available at wileyonlinelibrary.com.]

shows similar trend with M_H. The increase in crosslinks produced similar increment in modulus, which was consistent with the observed increment in modulus at 100% elongation (M_{100}) and modulus at 300% elongation (M_{300}) in this study.

The effects of ENR-50 and temperature on the tensile strength of NR/EPDM blends are shown in Figure 2(a). Tensile strength increased with the increase of ENR-50 in the blends. This may be due to the improved interaction between NR and EPDM with the presence of polar groups in ENR-50 and enhanced distribution of EPDM in the NR matrix.[33] This behavior is in line with SEM observation as shown in Figure 5.

M_{100} and M_{300} are the measures of rubber stiffness.[34] The effect of ENR-50 on the tensile modulus (M_{100} and M_{300}) of NR/EPDM blends is depicted in Figure 2(b,c), respectively. M_{100} and M_{300} increased as ENR-50 content increased. The incorporation of ENR-50 into rubber matrix increased the rigidity of vulcanizates.[35] This strongly correlates with the presence of epoxide groups in ENR-50 which efficiently hinders the chain sliding past one another when the material is placed under tension.[36] As a result, it could hold them together and increase their resistance to deformation. This helps in improving modulus of the composites. Rotor speed also exerted some influence on the tensile modulus. Figure 2(b,c) shows that the value of M_{100} and M_{300} decrease when rotor speed increases. Notably, high rotor speed at very high temperature is not recommended, because it will result in a yellowish compound due to the effect of polymer degradation. This is caused by strong shearing forces and shear viscous heat which would intensify the damaging of the rubber chain by mechanical shear stress. Meanwhile, too slow rotor speed may cause excessively long mixing cycles and not economical for processing. Thus, an appropriate rotor speed is essential to improve the dispersion of dispersed phases within matrix and consequently increase the mechanical properties.[37]

Figure 2(d) shows the effect of ENR-50 on elongation at break (E_B) of NR/EPDM blends. The E_B increased as ENR-50 content increased. The ENR-50 acted as anchor points between NR and EPDM chains, and postponed the premature behavior by preventing chain slippage from occurring. Thus, it allowed the blends to be extended to higher degree compared to neat NR/EPDM blends.

The predicted tensile strength at each experimental point is given in Table V along with the experimental data. The regression model (see Table IV) is accurate in describing and predicting the pattern of significance for the tensile strength. The low

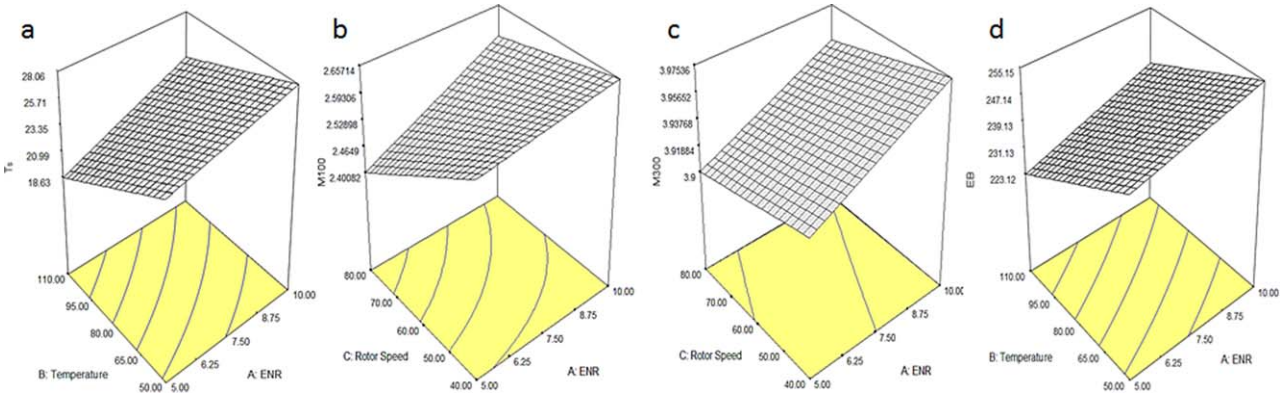

Figure 2. Response surface plot showing variation in (a) tensile strength (Ts); (b) modulus at 100% elongation (M_{100}); (c) modulus at 300% elongation (M_{300}); and (d) elongation at break (E_B). [Color figure can be viewed in the online issue, which is available at wileyonlinelibrary.com.]

Table V. Comparisons of Experimental and Predicted Tensile Strength Values of NR/EPDM Blends

Experiments	Experimental value (*Y*; MPa)	Predicted value (*Y*; MPa)
1	22.69	22.23
2	23.85	24.31
3	19.01	19.47
4	26.64	26.18
5	24.95	25.20
6	27.98	27.73
7	19.76	19.52
8	21.71	21.96
9	26.72	27.18
10	31.93	31.47
11	18.93	18.47
12	26.93	27.39
13	26.18	25.94
14	28.49	28.74
15	16.83	17.08
16	20.02	19.77
17	30.01	30.07
18	30.01	30.07
19	30.18	30.07

ENR-50 content with high temperature, rotor speed, and mixing time resulted in a nonuniform mixture that reduced the tensile strength, as represented by experiment No. 15 (coded as *R*15). Conversely, the maximum value of tensile strength was obtained at high ENR-50 content and high mixing time. It was observed in experiment No. 10 (coded as *R*10) with low mixing temperature and low rotor speed. The samples for best and worst mixing parameters were later compared with neat NR/EPDM labeled as *R*0 to be further analyzed through swell measurement, DSC, and SEM to support the mathematical and statistical analyses generated by the software.

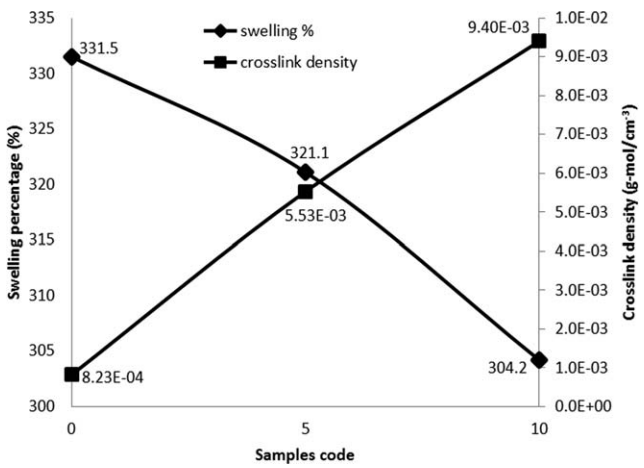

Figure 3. The swelling percentage and crosslink density of the NR/EPDM blends.

Table VI. DSC Results Obtained for Neat Rubbers with Their Blends

Blends	T_g (°C)
Neat NR	−10.73
Neat EPDM	−51.76
Neat ENR-50	−24.10
Neat NR/EPDM (*R*0)	−50.67, −22.71
*R*15	−11.11, −50.72
*R*10	−51.30

Experimental Analysis on NR/EPDM Blends

Swelling Behavior. Swell measurements were conducted to determine the crosslink density of NR/EPDM blends respective to the combination effects of ENR-50 content and mixing parameters. The toluene uptake and crosslink density of NR/EPDM blends for *R*0, *R*10, and *R*15 sample are shown in Figure 3. It is widely accepted that the toluene uptake is directly correlated to the crosslink density of a network chain, whereby less solvent penetrate through the blends indicating higher crosslink density.[33] From the plot, it can be observed that the toluene uptake for *R*10 was lower than *R*15. This could be reasonably attributed to the increased interaction between NR and EPDM with the presence of polar group in ENR which resembled a three dimensional network in the blends. The networks restricted the capability of the blends to absorb toluene since there were less open chains and gaps between rubber molecules for the toluene to penetrate.[32] The decreased toluene uptake was indirect representation of increased crosslink density in sample *R*10 as compared to *R*15. This observation is in line with the increment in blend stiffness due to restriction to molecular motion of the blend chains by crosslinks as previously discussed in tensile properties.

DSC Analysis. Compatibility of a rubber blends can be determined by DSC analysis which measures the glass transition temperature (T_g) and melting temperature (T_m) of a material. According to Rao and Johns,[38] a single and sharp peak indicates a highly miscible blend. Meanwhile, intermediate peak with value between those of the constituent components show a partial miscible blend and separated peak indicates an immiscible blend. The thermal characteristics of NR, EPDM, ENR-50 and their blends were examined by DSC in the temperature ranging from −65 to 100°C which allowed the identification of glass transition temperatures, T_g. Table VI features the T_g values for neat NR, EPDM, ENR and their blends while Figure 4 illustrates the scan traces of the DSC thermogram. Neat NR/EPDM blends (*R*0) was an immiscible blend with two distinct glass transitions region observed in its DSC curve. Meanwhile, high temperature, high rotor speed, and low mixing time led to phase separation due to thermal degradation and chains breakage.[39] Hence, *R*15 exhibited two distinct T_g values corresponding to the two neat constituents for the blend compositions.

Conversely, DSC thermogram of *R*10 exhibited single T_g curve in both NR/EPDM constituent blends where T_g for the blends was clearly seen as sharp peaks, indicating improved compatibility of NR/EPDM phases. Besides, the mean T_g value of neat NR

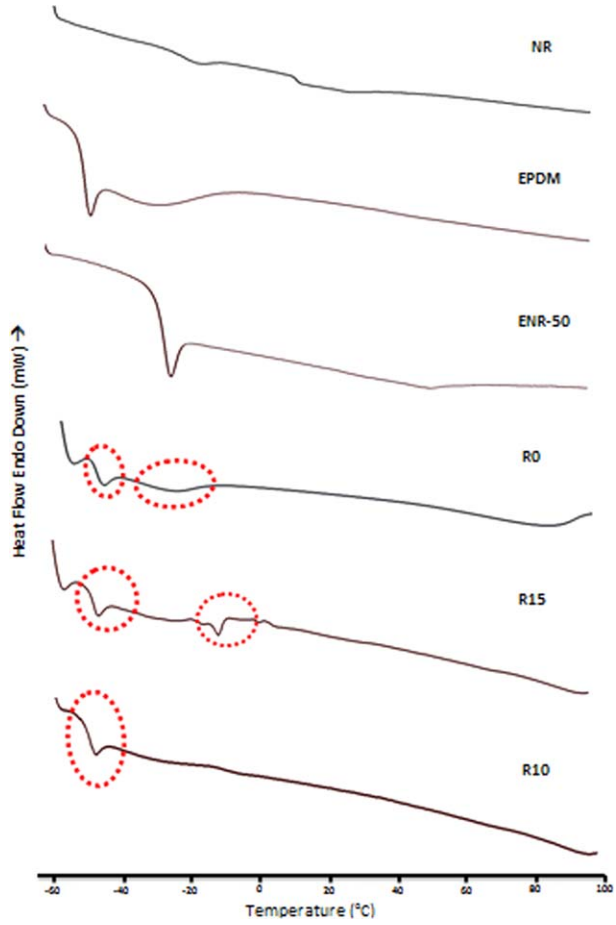

Figure 4. DSC thermograms of neat rubbers with *R*0, *R*15, and *R*10. [Color figure can be viewed in the online issue, which is available at wileyonlinelibrary.com.]

and EPDM shifted in this blend. This may result from some interaction between NR and EPDM at the boundaries of their phases forming a third phase.[40] The combination effects of compatibilizers and processing parameters were able to create a well-dispersed discontinuous phases that exhibited rheological properties almost similar to those obtained for compatible blends having one glass transition. This is in agreement with Asaletha et al.[41] study, which indicates that the main role of compatibilizer is to act as an interfacial agent in the immiscible blends. According to them,[41] if two polymers are far from being miscible, then no copolymer is likely to make a one-phase system.

SEM Analysis. Figure 5 illustrates the SEM micrographs taken from the tensile fracture surfaces of *R*0, *R*15, and *R*10 at magnification of 300×, respectively. The morphological characteristics of NR/EPDM blends for specific processing parameters and ENR contents depicted the physical and mechanical properties of the blend. *R*10 (Figure 5c) exhibited much rougher surfaces with many tear lines compared to *R*0 and *R*15 [Figure 5(a,b)], which displayed broader tearing lines between phases. These explained good interaction and better stress transfer across the interface between the NR and EPDM matrix occurred in *R*10 sample. The uniform dispersion of EPDM in the NR matrix altered the crack paths which led to a higher resistance to crack propagation and, hence, higher tensile strength.

CONCLUSIONS

In conclusion, the interaction between mixing parameters established by the RSM is consistent with microstructure and material properties of the samples. The incorporation of ENR-50 into NR/EPDM blends enhances the compatibility and improves rheological properties of rubber blends; while mixing temperature, rotor speed, and mixing time also contribute to the improvement in miscibility between NR and EPDM. In this study, the coefficient of determination (R^2) is sufficient to represent model fit between experimental and predicted value by the software. Hence, the generated regression model can be utilized to optimize compatibilizer contents and processing parameters for producing the NR/EPDM blends at optimum properties. The aim to investigate the effects of processing

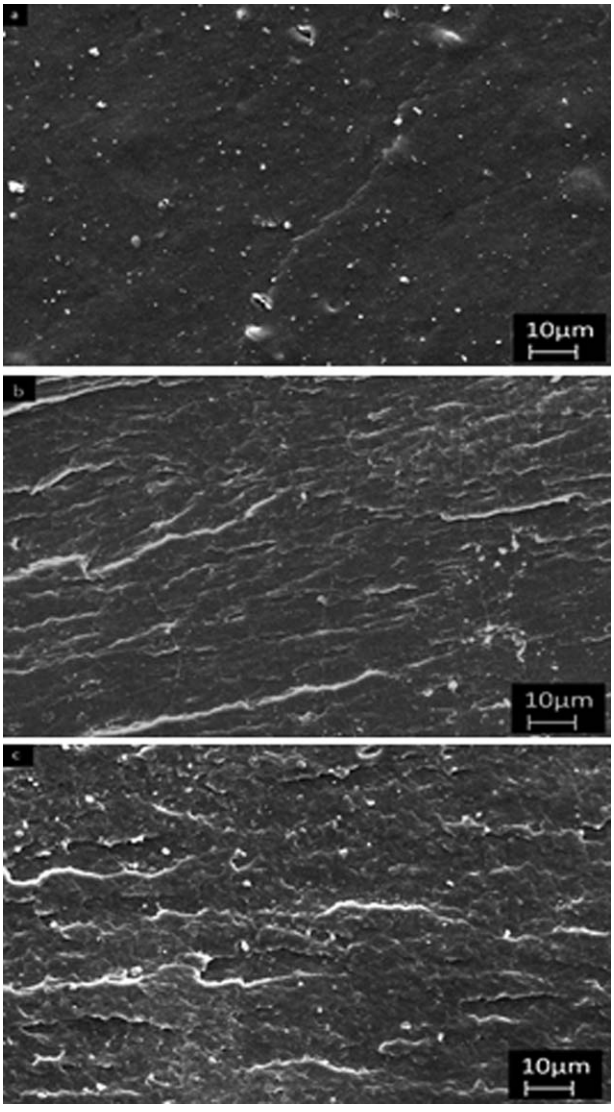

Figure 5. SEM micrographs showing tensile fracture surface of NR/EPDM blends at 70/30 blend ratio: (a) *R*0, (b) *R*15, and (c) *R*10 at 300× magnifications.

conditions (temperature, rotor speed, and time) and presence of ENR-50 is thus verified. The findings can be summarized as follows:

1. The incorporation of ENR-50 as compatibilizer in NR/EPDM blends enhances the scorch time, maximum torque, torque difference, tensile strength, tensile modulus, elongation at break, and swelling resistance of the blends respective to optimum processing parameters.
2. The cure time of NR/EPDM blends decrease as ENR-50 content increases together with temperature factors in the blends.
3. DSC results reveal that *R*10 shows a single and sharp T_g peak with a suitable combination of mixing parameters which correspond to a miscible blend.
4. The tensile fracture surfaces of compatibilized NR/EPDM blends (*R*10) indicate a better dispersion and stronger interfacial adhesion between NR and the EPDM matrix. In contrast, neat NR/EPDM blends and *R*15 show a fairly smooth fracture surfaces due to a lower adhesion between NR and the EPDM matrix which usually indicates a low compatibility accompanied with a premature, rather brittle-type failure.

ACKNOWLEDGMENTS

The authors acknowledge the Ministry of Education Malaysia for funding this research through the Fundamental Research Grant Scheme (FRGS/2012/FKP/TK04/02/1 F00132). The authors thank the UTeM and Malaysia Nuclear Agency which provided the expertise, equipment, and technical assistance while the authors conducted the experiments.

REFERENCES

1. Botros, S. *Polym. Plast. Technol. Eng.* **2002**, *41*, 341.
2. Utracki, L. Commercial Polymer Blends; Kluwer Academic Publishers: London, **1998**.
3. Ismail, H.; Shaari, S.; Othman, N. *Polym Test.* **2011**, *30*, 784.
4. Boonsong, K.; Seadan, M.; Lopattananon, N. *Songklanakarin J. Sci. Technol.* **2008**, *30*, 491.
5. Alipour, A.; Naderi, G.; Ghoreishy, M. H. *J. Appl. Polym. Sci.* **2013**, *127*, 1275.
6. Cancarb. Properties of Thermal Black Filled EPDM Engine Mount; Technical bulletin 019: Canada, **1999**.
7. Mastromatteo, R.; Mitchell, J.; Brett, T, Jr. *Rubber Chem. Technol.* **1971**, *44*, 1065.
8. Singh, D.; Malhotra, V.; Vats, J. *J. Appl. Polym. Sci.* **1999**, *71*, 1959.
9. Oommen, Z.; Thomas, S. *J. Appl. Polym. Sci.* **1997**, *65*, 1245.
10. Arayapranee, W.; Rempel, G. L. *J. Appl. Polym. Sci.* **2008**, *109*, 932.
11. Pasbakhsh, P.; Ismail, H.; Fauzi, M.; Bakar, A. A. *Polym Test.* **2009**, *28*, 548.
12. Oliveira, M. G.; Soares, B. G. *J. Appl. Polym. Sci.* **2001**, *82*, 38.
13. Sirqueira, A. S.; Soares, B. G. *J. Appl. Polym. Sci.* **2002**, *83*, 2892.
14. Lewis, C.; Bunyung, S.; Kiatkamjornwong, S. *J. Appl. Polym. Sci.* **2003**, *89*, 837.
15. Tedesco, A.; Barbosa, R. V.; Nachtigall, S. M. B.; Mauler, R. S. *Polym Test.* **2002**, *21*, 11.
16. Chang, Y. W.; Shin, Y. S.; Chun, H.; Nah, C. *J. Appl. Polym. Sci.* **1999**, *73*, 749.
17. Tanrattanakul, V.; Sungthong, N.; Raksa, P. *Polym Test.* **2008**, *27*, 794.
18. Arroyo, M.; Lopez-Manchado, M.; Valentin, J.; Carretero, J. *Compos. Sci. Technol.* **2007**, *67*, 1330.
19. Teh, P.; Mohd Ishak, Z.; Hashim, A.; Karger-Kocsis, J.; Ishiaku, U. *Eur. Polym. J.* **2004**, *40*, 2513.
20. Margaritis, A. G.; Kalfoglou, N. K. *Polymer* **1987**, *28*, 497.
21. Noriman, N.; Ismail, H.; Rashid, A. *Polym Test.* **2010**, *29*, 200.
22. Barick, A. K.; Jung, J. Y.; Choi, M. C.; Chang, Y. W. *J. Appl. Polym. Sci.* **2012**, *129*, 1405.
23. Mohamad, N.; Muchtar, A.; Ghazali, M. J.; Mohd, D. H.; Azhari, C. H. *J. Appl. Polym. Sci.* **2010**, *115*, 183.
24. Khuri, A. I.; Cornell, J. A. Response Surfaces: Designs and Analyses. Vol. *152*; CRC press: New York, **1996**.
25. Nassiri, H.; Arabi, H.; Hakim, S.; Bolandi, S. *Polym. Bull.* **2011**, *67*, 1393.
26. Bas, D.; Ismail, H.; Boyaci, J. *J. Food Eng.* **2007**, *78*, 836.
27. Raissi, S.; Farsani, R. E. *World Acad Sci Eng Technol* **2009**, *51*, 267.
28. Kukreja, T.; Kumar, D.; Prasad, K.; Chauhan, R.; Choe, S.; Kundu, P. *Eur. Polym. J.* **2002**, *38*, 1417.
29. Annual Book of ASTM Standards; American Society for Testing of Materials: West Conshohocken, PA, **2001**.
30. Ghasemi, I.; Karrabi, M.; Mohammadi, M.; Azizi, H. *Express Polym Lett.* **2010**, *4*, 62.
31. Sommer, J. G. Engineered Rubber Products: Introduction to Design, Manufacture and Testing; Hanser Verlag: Munich, **2009**.
32. Sadequl, A.; Ishiaku, U.; Ismail, H.; Poh, B. *Eur. Polym. J.* **1998**, *34*, 51.
33. Mittal, V.; Kim, J. K.; Pal, K. Recent Advances in Elastomeric Nanocomposites. Vol. *9*; Springer: Berlin, **2011**.
34. Mohamad, N.; Muchtar, A.; Ghazali, M. J.; Mohd, D. H.; Azhari, C. H. *J. Elastomers Plast.* **2010**, *42*, 331.
35. Mohamad, N.; Muchtar, A.; Ghazali, M. J.; Mohd, D. H.; Azhari, C. H. *Eur. J. Sci. Res.* **2008**, *24*, 538.
36. Mousa, A.; Karger-Kocsis, J. *Macromol. Mater. Eng.* **2001**, *286*, 260.
37. Afifi, H. A.; El Sayed, A. M. *Polym. Bull.* **2003**, *50*, 115.
38. Utracki, L. A. Polymer Blends Handbook; Kluwer Academic Publishers: London, **2002**.
39. Rao, V.; Johns, J., *J. Therm. Anal. Calorim.* **2008**, *92*, 801.
40. Tincer, T.; Coskun, M. *Polym. Eng. Sci.* **1993**, *33*, 1243.
41. Asaletha, R.; Kumaran, M.; Thomas, S. *Polym. Degrad. Stab.* **1998**, *61*, 431.